Zhao JL, Wu ZK, Pan ZK *et al.* 3D face similarity measure by Fréchet distances of geodesics. JOURNAL OF COMPUTER SCIENCE AND TECHNOLOGY 33(1): 207–222 Jan. 2018. DOI 10.1007/s11390-018-1814-7

3D Face Similarity Measure by Fréchet Distances of Geodesics

Jun-Li Zhao[1,2], *Member, CCF*, Zhong-Ke Wu[3], *Member, CCF*, Zhen-Kuan Pan[4,*], *Member, CCF*
Fu-Qing Duan[3], *Member, CCF*, Jin-Hua Li[1], *Member, CCF*, Zhi-Han Lv[1]
Kang Wang[5], and Yu-Cong Chen[3]

[1]*School of Data Science and Software Engineering, Qingdao University, Qingdao 266071, China*
[2]*College of Automation and Electrical Engineering, Qingdao University, Qingdao 266071, China*
[3]*College of Information Science and Technology, Beijing Normal University, Beijing 100087, China*
[4]*College of Computer Science and Technology, Qingdao University, Qingdao 266071, China*
[5]*School of Management, Capital Normal University, Beijing 100048, China*

E-mail: zhaojl@yeah.net; zwu@bnu.edu.cn; zkpan@126.com; fqduan@bnu.edu.cn; lijh@qdu.edu.cn
lvzhihan@gmail.com; {wangkang-1984, lionelclark}@163.com

Received June 20, 2017; revised December 9, 2017.

Abstract 3D face similarity is a critical issue in computer vision, computer graphics and face recognition and so on. Since Fréchet distance is an effective metric for measuring curve similarity, a novel 3D face similarity measure method based on Fréchet distances of geodesics is proposed in this paper. In our method, the surface similarity between two 3D faces is measured by the similarity between two sets of 3D curves on them. Due to the intrinsic property of geodesics, we select geodesics as the comparison curves. Firstly, the geodesics on each 3D facial model emanating from the nose tip point are extracted in the same initial direction with equal angular increment. Secondly, the Fréchet distances between the two sets of geodesics on the two compared facial models are computed. At last, the similarity between the two facial models is computed based on the Fréchet distances of the geodesics obtained in the second step. We verify our method both theoretically and practically. In theory, we prove that the similarity of our method satisfies three properties: reflexivity, symmetry, and triangle inequality. And in practice, experiments are conducted on the open 3D face database GavaDB, Texas 3D Face Recognition database, and our 3D face database. After the comparison with iso-geodesic and Hausdorff distance method, the results illustrate that our method has good discrimination ability and can not only identify the facial models of the same person, but also distinguish the facial models of any two different persons.

Keywords 3D face, similarity measure, Fréchet distance, geodesic

1 Introduction

With the popularity of three-dimensional (3D) scanning device, it is increasingly convenient to achieve high-precision 3D facial data. 3D human faces have emerged as an active research topic in computer vision and computer graphics fields[1]. Shape analysis and similarity measure of 3D facial surface have become hot topics, which have important applications in face recognition, 3D facial reconstruction, facial surgery, 3D animation, biometrics, forensic and other fields.

Generally similarity is an ambiguous and relative concept for human beings[2]. The similarity between two objects is often different when it is judged by different people, which depends on the perception and experiences of each person. Therefore, similarity measure is a difficult problem. Especially, human face similarity is more difficult to measure since human faces are glob-

Regular Paper

This work was supported by the National Natural Science Foundation of China under Grant Nos. 61702293, 61772294, and 61572078, the Open Research Fund of the Ministry of Education Engineering Research Center of Virtual Reality Application of China under Grant No. MEOBNUEVRA201601. It was also partially supported by the National High Technology Research and Development 863 Program of China under Grant No. 2015AA020506, and the National Science and Technology Pillar Program during the 12th Five-Year Plan Period of China under Grant No. 2013BAI01B03.

*Corresponding Author

ally similar in terms of main physical features (eyes, mouth, nose, etc). We can only distinguish two faces by details.

Currently few papers are involved in 3D facial similarity measure, and most researchers adopt subjective evaluation methods. Stephan and Arthur[3] and Quatrehomme *et al.*[4] invited several respondents to judge the facial similarity. Although this evaluation method is consistent with human cognitive theory, the evaluation process requires a lot of manpower and time, and the accuracy of the evaluation is influenced by human subjective factors. Therefore, an objective similarity measure method is needed. Only a few researchers conducted preliminary exploration on this problem with objective methods. Li *et al.*[5] extracted the iso-geodesic stripes to measure the similarity. They described each pair of stripes by a distribution vector of 12 dimensions and computed similarity based on the space distribution vectors. Moorthy *et al.*[6] took Gabor features as the similarity measure standard, which are extracted from automatically detected feature points on the range and texture images of 3D faces. And they also compared objective similarity with subjective study results.

The related researches of 3D face similarity focus mostly on face recognition which is to identify a face from a given face database. 3D face similarity measure is to compare 3D facial models represented by computers through a certain method and obtain their similarity value. As face similarity measure research is closely related to 3D face recognition, we introduce some research work in which the face recognition methods are close to our method as follows.

Most of 3D face recognition methods recognize faces by extracting the geometrical characteristics of the face model, including face feature points, facial curves, facial surface and so on. The method based on facial curves is the closest to our method. Therefore, here we describe the related work of the method in detail and other work about face recognition can be found in [7-8]. Nagamine *et al.*[9] presented a human face identification method and they observed that facial central axis, and nose and mouth features have the major distinctiveness. Wu *et al.*[10] addressed face authentication based on multiple profiles extracted from range data, including central profile, nose-crossing profile and forehead-crossing profile. ter Haar and Veltkamp[11] computed the similarity of 3D faces using a set of eight contour curves. Jahanbin *et al.*[12] proposed a personal identity verification framework based on extracted iso-depth and iso-geodesic curves from facial surfaces. Due to geodesics' intrinsic and good properties, it has been widely used in 3D face shape analysis and recognition recently. Bronstein *et al.*[13] assumed that 3D facial models of different facial expressions can be regarded as isometric transformation, under which geodesic distance is preserved. Therefore, they investigated 3D face shape analysis and recognition by a variety of methods based on geodesic distances. Berretti *et al.*[14-15] proposed a face recognition method by the spatial distribution features of the facial iso-geodesic stripes. Mpiperis *et al.*[16] used a geodesic polar parameterization for face representation and face recognition. Their methods mainly utilize geodesic distances for face recognition, but they did not take advantage of geodesics.

Similarity is usually measured through distances between some extracted features, vectors or their combinations[2]. Achermann and Bunke[17] classified range images of human faces with Hausdorff distance. Wu *et al.*[10] used a global profile matching approach based on the partial Hausdorff metric to align and compare profiles. Lee and Shim[18] implemented human face verification based on depth-weighted Hausdorff distance (DWHD) whose weighting function is based on depth values. Jahanbin *et al.*[12] encoded facial characteristics by several features like the shape descriptor or polar Euclidean distance from the nose tip.

Although the Hausdorff distance is arguably a natural distance measure between curves or compact sets, it considers neither the direction nor any dynamics of the motion along the curves. The Fréchet distance takes the order between points along the curves into consideration, which makes it a better measure of curves similarity than its alternatives[19].

Through introducing Fréchet distance, this paper proposes a 3D human face similarity measure method based on Fréchet distances of geodesics on 3D facial models. Our similarity measure method has two merits. 1) Geodesic is intrinsic and invariant with the representation. And the geodesic distance between two points on the surface is preserved under isometric deformation. Compared with general curves, a geodesic is insensitive to the variation of the expression; therefore we select geodesics as the comparison curves. 2) Fréchet distance is an effective metric for measuring curve similarity because it takes the order between points along the curves into consideration, which can capture the similarity of curves better than other similarity measures such as the Euclidean distance and the Hausdorff distance. Therefore we choose it to measure 3D face similarity.

2 Geodesic Representation of 3D Facial Models

The basic assumption of our method is that a facial surface f can be represented as a 2D Riemannian manifold embedded in $\mathbb{R}^3$, which is compact, connected and zero-genus. And the two facial surfaces f_1 and f_2 of the same person in the presence facial expressions are isometric, i.e., there is a diffeomorphism $m : f_1 \rightarrow f_2$ which takes curves in f_1 to curves of the same length in f_2. The assumption that facial expressions can be modeled as isometrics of the facial surface was proposed by Bronstein *et al.*[13] Under the assumption, as an intrinsic geometry quantity, the geodesic which is deduced by Riemannian metric can be used to construct expression-invariant representation of faces. And geodesic distance $d_f(p_i, p_j)$ on f for $p_i, p_j \in f$ induced by the Riemannian metric is preserved under two facial surfaces of different expressions, i.e., $d_{f_1}(p_i, p_j) = d_{f_2}(\phi(p_i), \phi(p_j))$. Because a geodesic is an intrinsic geometry quantity and is not sensitive to expressions, 3D face similarity measure can be computed by comparing the similarity of extracted corresponding geodesics on them, which is measured by Fréchet distance in this paper.

The main contribution of this paper is to introduce geodesic and Fréchet distance to measure 3D face similarity for the first time. By computing Fréchet distance of geodesics extracted from 3D facial models, the surface comparison of 3D faces is converted into 3D curves comparison on the facial surfaces. Firstly, the geodesics on each 3D facial model emanated from the nose tip point are extracted in the same initial direction with equal angular increment. Secondly, the Fréchet distances of the corresponding geodesics on the two compared facial models are computed. Finally, the similarity of two facial models is computed based on the Fréchet distances of the geodesics.

2.1 Preprocessing of 3D Facial Models

The 3D facial data acquired by a 3D scanner or other devices often have problems such as holes, gaps, degeneracies or non-manifold configurations. Therefore we firstly need to fill holes and gaps, delete the scattered points, and repair the incomplete part of the models in order to make a 3D facial model to be a complete triangular mesh model and well-structured manifold. Secondly, the 3D face models will be normalized and unified to a coordinate system in order to eliminate the effects of data scale or posture. Thirdly, all facial models are cut by the same reference face model and registered by the non-rigid data registration method[20] in order to eliminate the effects of translation, rotation and so on.

2.2 Encoding Face Geometry by Geodesics

A geodesic is a curve with zero geodesic curvature, which is a local shortest curve between two points on a surface. A geodesic is intrinsic and is invariant with the representation. Under isometric transformation, the geodesic distance which is the length of the shortest geodesic between two points is preserved. Geodesic is an intrinsic geometry quantity, which is deduced by Riemannian metric. Bronstein *et al.*[13] proved that the geodesic distance is more stable than the Euclidean one under facial expression variations through placing 133 markers on a face and computing the distances between these points under facial expressions deformations. Under small facial expressions deformations, the two facial surfaces of the same person in the presence facial expressions can be seen as isometric. Consequently, the geodesic distance between two points on the surface is preserved and the geodesic is also preserved.

Our method makes full use of geodesic properties to construct expression-invariant representation of faces. Compared with general curves, the geodesic is insensitive to the variation of the expression. It can be used in the field of 3D face recognition and analysis invariant to expressions. Thus we encode face geometry by geodesics in expression-invariant face similarity measure.

2.3 Extracting Geodesics on 3D Facial Models

The first step is to determine the source point of geodesics. The tip point of a nose, located at the center of the whole face, takes an important role in face shape, and is easy to locate. Therefore the tip point of nose is selected as the source point of all geodesics because of its physiological feature and its location. In the standard posture, the tip point of a nose is the highest point of the face. Accordingly, it can be located by finding the point with maximum y value as the nose tip point (O) on the 3D face model under standard posture. Through this method, the tip point of a nose is robust. Thus the nose tip point which is found by the above method is taken as the source point of all geodesics.

The second step is to locate the target points of geodesics. In order to eliminate the effects of irregular boundary points, all extracted geodesics are located within the outermost iso-geodesic. Thus the target points will be found on the outermost iso-geodesic, which is extracted by the following steps. Firstly, the boundary of the 3D facial model is extracted. Secondly the geodesic distances from the nose tip to all boundary points of the facial model are computed. Finally the shortest geodesic distance from the nose tip to all the boundary points of the facial model is found and the outermost iso-geodesic (denoted by IG) is extracted according to the shortest geodesic distance.

In order to make the geodesics distributed evenly and geodesics on two models become corresponding curves, geodesics are extracted with the same initial direction and equal angular increment. The same initial direction is determined by the first target point and the source point. The first target point is located in the outermost iso-geodesic (IG) and its x-coordinate is the same with that of the nose tip point in the standard pose of the preprocessed facial models. The geodesic connecting these two points can divide a face into two parts. Thus, this geodesic is taken as the initial geodesic, i.e., the first geodesic.

The other equal division points on the outermost iso-geodesic are obtained by equal angle increment. Since the iso-geodesic is not a plane curve, we project it into a tangent plane of the nose tip point so that the equal angle intervals can be easily obtained.

In the standard pose of 3D facial models which have been preprocessed and aligned, and whose coordinate systems have been united, the tangent plane is the plane where the points have the equal y coordinates. In order to simplify the calculation, firstly we build a coordinate system taking the nose tip as the origin point. Then all points' coordinates are transformed into the new coordinate. Thus, the tangent plane can be found by the equation $y = 0$. Through this projection, the tangent plane is unique and stable.

On the tangent plane, the lines from the nose tip point to the projected outermost iso-geodesic are computed by a certain angular increment, and the intersection points between these lines with the projected outermost iso-geodesic IG$'$ are obtained. The intersection points are projected into the original outermost iso-geodesic IG and the equal angular increment points are obtained. These points are described by the following formula:

$$P = \cup_{\alpha} p_a (\alpha \in A),$$

$$A = \{0, \frac{2\pi}{m}, \frac{4\pi}{m}, \cdots, \frac{2\pi(n-1)}{m}\},$$

where p is a equal division point, i.e., equal angular increment point, $\cup$ represents union, $\cup_{\alpha}$ represents the union of angular equal division points with α angular increment, P is a set of all equal division points, A is the set of all angular, n is the number of angular, m is the number of the equal division points and equal to the number of geodesics, and α is the equal angular increment. And these equal division points are taken as target points of geodesics. Fig.1 shows the equal division points.

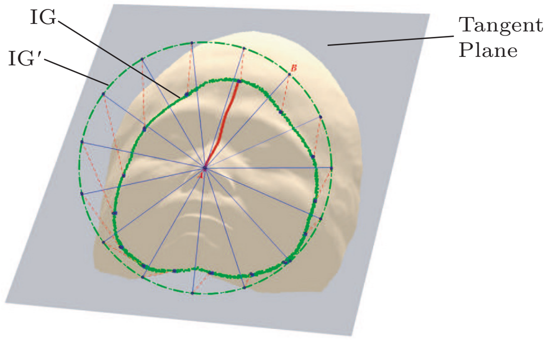

Fig.1. Locating the equal division points on the outermost iso-geodesic.

The third step is computing the geodesics from the nose tip point to the equal division points on the outermost iso-geodesic. This can be realized by the geodesic algorithm of single-source-multi-destination. The compared 3D facial model is assumed to be the complete triangular mesh model, which can be seen as a connected manifold surface. Geodesics can be computed by the MMP[21], ICH[22], PCH[23], SVG[24] algorithm, etc. The classic MMP algorithm[21] is used in our method. In the MMP algorithm geodesics on triangle mesh surface are solved according to the principle that light propagates along straight lines. In 2005, Surazhsky *et al.*[25] gave an implementation of the MMP algorithm. In the MMP algorithm, a window function is defined firstly and then windows are generated. The positions of the pseudo-sources are calculated based on the windows, and then the geodesic distance from any point to the source point on the model can be calculated through the windows. Geodesics can be obtained by backtracking. The first point of the geodesics can be found by finding the point with the shortest geodesic distance on all windows of the triangular face where the point is. The other points of geodesics can be found by traveling the adjacent windows in turn.

The extracted m geodesics with equal angular increment α on 3D facial models according to the above geodesic extracting method in Subsection 2.3 can be denoted by the following equations:

$$G = \cup_\alpha g_\alpha (\alpha \in A),$$
$$A = \{0, \frac{2\pi}{m}, \frac{4\pi}{m}, \cdots, \frac{2\pi(n-1)}{m}\},$$

where G indicates the set of geodesics, and A denotes a set of geodesic angles. In Fig.2, 60 geodesics which we extract from two 3D facial models are shown.

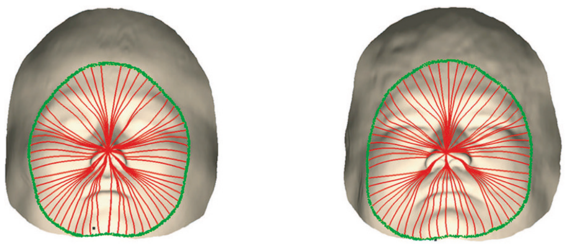

(a) (b)

Fig.2. Geodesics on two 3D facial models. (a) Facial model f_1. (b) Facial model f_2.

The algorithm of extracting geodesics from 3D facial models is shown in Algorithm 1.

Algorithm 1. Extracting Geodesics

Input: 3D facial model

Output: geodesics G

Locate the nose tip point O

Extract the boundary B of 3D facial model

Compute the geodesic distance from O to all points on B and find the shortest geodesic distance

Extract the outmost iso-geodesic IG by the shortest geodesic distance

Project IG onto 2D tangent plane, and get IG′

Find the geodesic connected with the nose tip point and the point with the same x-coordinate with the nose tip point as the first geodesic

For $\alpha = 0$ to 2π **do**

  Locate the equal angular division points p'_α on IG′

  Project the equal division points p'_α on IG′ onto 3-dimensional iso-geodesic IG and get p_α

  Compute geodesic $g_\alpha = geodesic(O, p_\alpha)$

End

Return $G = \cup_\alpha g_\alpha (\alpha \in A)$

3 Computing Fréchet Distances of Corresponding Geodesics

The Fréchet distance is a metric to measure the similarity of curves and is better than the Hausdorff distance for measuring the similarity between two curves. It was firstly proposed by Fréchet[26] in 1906 and firstly applied into the similarity measure of polygon curves by Alt and Godau[27] in early 1990s. Fréchet distance can be interpreted as the minimum-length leash required of two curves. The Fréchet distance between two curves is often referred to as a dog-leash distance because it can be interpreted as the minimum-length leash required for a person to walk with a dog, if each of the person and the dog travels from their respective starting position to their ending position, without ever letting go off the leash or backtracking. The length of the leash determines how similar the two curves are to each other: a short leash means that the curves are similar, and a long leash means they are different from each other.

The definition of Fréchet distance is as follows.

Definition 1 (Fréchet Distance[19]). *A monotone parameterization of* $[0, b]$ *is a continuous non-decreasing function* $\alpha : [0, 1] \to [0, b]$ *with* $\alpha(0) = 0$ *and* $\alpha(1) = b$. *Given two polygonal curves* M *and* N $(a, b > 0)$ *of lengths* a *and* b *respectively, the Fréchet distance between* M *and* N *is defined as*:

$$\delta_F(M, N) = \inf_{\alpha,\beta} \max_{t\in[0,1]} d(M(\alpha(t)), N(\beta(t))),$$

where d *is the Euclidean distance, and* α *and* β *range over all monotone parameterization of* $[0, b]$ *and* $[0, a]$, *respectively.*

Fig.3 gives an intuitive illustration of the Fréchet distance between two curves M and N.

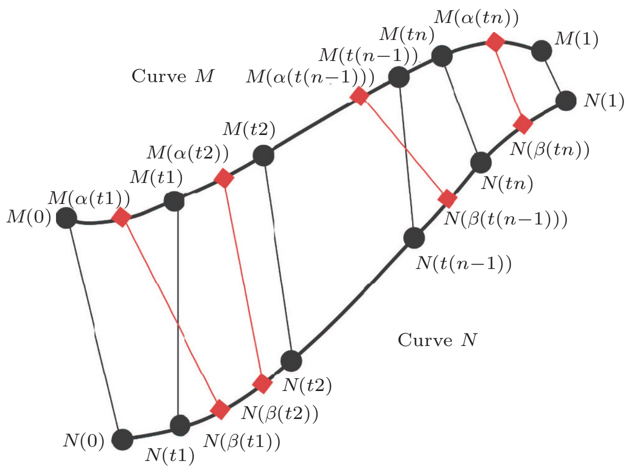

Fig.3. Illustration of the Fréchet distance between two curves M and N.

The Fréchet distance takes the order between points along the curves into consideration, which can capture the similarity of curves better than other similarity measures such as the Euclidean distance and the Hausdorff distance. The Hausdorff distance is arguably a natural distance measure between curves or compact sets, and it is too static in the sense that it considers neither the direction nor any dynamics of the motion along the curves. The most important difference between the Fréchet distance and the Hausdorff distance is that the Fréchet distance takes the order between points along the curves into consideration while the Hausdorff distance does not. We have demonstrated the above conclusion through computing the Hausdorff distance and the Fréchet distance of the two geodesics (the red curve and the blue curve in Fig.4(a)) on different people's faces.

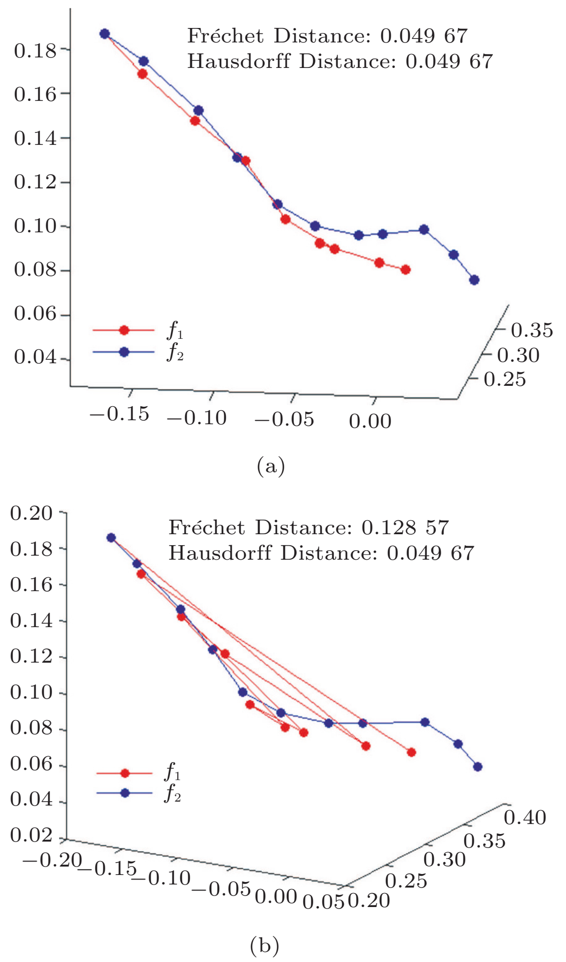

Fig.4. Hausdorff distance and Fréchet distance of the two geodesics. (a) Same. (b) Different.

In Fig.4(a) the Fréchet distance and the Hausdorff distance of the red curve and the blue curve are the same. In Fig.4(b) after we change the order of the points in the red curve and maintain the positions of the points unmoved, the Fréchet distance and the Hausdorff distance of the red curve and the blue curve are different, and the Fréchet distance is bigger than the Hausdorff distance. We can see from Fig.4: when we change the order of the points in the red curve, the red curve and the blue curve are not similar. This figure reveals the Fréchet distance can represent the similarity of the two curves better than the Hausdorff distance.

Alt and Godau[27] gave an exact algorithm for computing the Fréchet distance between two polygonal curves. Its time complexity is $O(mn\log^2 mn)$, where m and n are the number of vertices of the two polygonal curves respectively. Rote[28] gave a more general algorithm that works for piecewise smooth curves. The above two algorithms use complex parametric search techniques on free space diagrams[27-28] and their complexity can be quite high in practice. Approximations to continuous Fréchet distance have been developed. Eiter and Mannila[29] proposed a discrete variation method of computing Fréchet distance which is adopted in this paper. This method is based on all couplings between the endpoints of the line segments of polygonal curves and uses the distance of coupling to approximate Fréchet distance. They proved that the upper bound of the distance of coupling is Fréchet distance. The complexity of computing coupling is only $O(mn)$ and the method is very simple. Therefore, it is used in our facial similarity computation.

For computing the Fréchet distance between arbitrary curves, one typical method is to convert the curves into polygonal curves in order to approximate them. The discrete variation method proposed by Eiter and Mannila[29] is introduced in the following part of this section. The polygonal curve in $\mathbb{R}^d$ is a continuous function $C : [0, n] \to \mathbb{R}^d$ with $n \in \mathrm{N}$, such that for each $i \in \{0, \dots, n-1\}$, the restriction of C to the interval $[i, i+1]$ is affine (i.e., forming a line segment). The integer n is called the length of C. The sequence $C(0), \dots, C(n)$ of endpoints of the line segments of C is denoted by $\sigma(C)$. Let M and N be polygonal curves, $\sigma(M) = (a_1, \dots, a_p)$ and $\sigma(N) = (b_1, \dots, b_q)$ be the corresponding sequences respectively. A coupling L between M and N is a sequence:

$$(a_{x_1}, b_{y_1}), (a_{x_2}, b_{y_2}), \dots, (a_{x_m}, b_{y_m}).$$

The sequence is of distinct pairs from $\sigma(M) \times \sigma(N)$ such that $x_1 = 1$, $y_1 = 1$, $x_m = p$, $y_m = q$, and for all $i = 1, \dots, q$, $x_{i+1} = x_i$ or $x_{i+1} = x_i + 1$, and $y_{i+1} = y_i$ or $y_{i+1} = y_i + 1$. Thus a coupling is related to the order of the points in M and N. The length $\|L\|$ of the coupling L is the length of the longest link in L, that is,

$$\|L\| = \max_{i=1,\dots,m} d(a_{x_i}, b_{y_i}).$$

The discrete Fréchet distance of polygonal curves M and N is defined by (1).

$$\delta_{dF}(M, N) = \min\{\|L\| \,|L \in C(M, N)\}. \quad (1)$$

$C(M, N)$ is a coupling between M and N. It is proved by Eiter and Mannila[29] that δ_{dF} is a metric and it is the upper bound of δ_F. Thus we can use δ_{dF} to approximate δ_F. The distance of coupling δ_{dF} can be computed by dynamic programming recurrences. Algorithm 2 shows how to compute δ_{dF}.

Algorithm 2. Computing δ_{dF}

Input: polygonal curves $M = (a_1, \dots, a_m)$ and $N = (b_1, \dots, b_n)$
Output: distance $\delta_{dF}(M, N)$

```
d_{1,1} = ||a_1 − b_1||_2
For j = 2 to n
  d_{1,j} = max{d_{1,j−1}, ||a_1 − b_j||_2}
For i = 2 to m
  d_{i,1} = max{d_{i−1,1}, ||a_i − b_1||_2}
For i = 2 to m
  For j = 2 to n
    d_{i,j} = max{min{d_{i,j−1}, d_{i−1,j}, d_{i−1,j−1}}, ||a_i − b_j||_2}
Return d_{m,n}
```

In the above algorithm, $\delta_{dF}(M, N)$ is given by $d_{m,n}$. Since $d_{i,j}$ represents the discrete Fréchet distance between the sub-curve $M|_{[1:i]}$ of M and the sub-curve $N|_{[1:j]}$ of N, $d_{m,n}$ represents the discrete Fréchet distance between the two entire curves. Time complexity of Algorithm 2 is $O(mn)$, which is lower than the complicated algorithms[27-28].

4 3D Facial Similarity Measure by Fréchet Distances of Geodesics

After the facial models have been preprocessed according to the method described in Section 2, geodesics can be extracted from the compared facial models using the method in Section 2. Thus the 3D facial surface can be represented by these geodesics approximately and the similarity measure of 3D surface is converted into the similarity measure of 3D curves. Furthermore, the corresponding geodesics extracted from two 3D facial models can be compared by the Fréchet distances and the similarity of two faces can be computed by the average of Fréchet distances of all corresponding geodesics.

Let f_1 and f_2 be two 3D facial models. m geodesics emanated from the nose tip point with the same initial direction and equal angular increment α on each model can be extracted. The angular index of geodesics is $A = \{0, \frac{2\pi}{m}, \frac{4\pi}{m}, \cdots, \frac{2\pi(n-1)}{m}\}$. Therefore, the sets of geodesics extracted from the two facial surfaces can be expressed as $G_1 = \cup_\alpha g^1_\alpha(\alpha \in A)$ and $G_2 = \cup_\alpha g^2_\alpha(\alpha \in A)$.

These geodesics can be used to represent 3D facial surface approximately:

$$f_1 \approx \cup_\alpha g^1_\alpha(\alpha \in A) \text{ and } f_2 \approx \cup_\alpha g^2_\alpha(\alpha \in A).$$

Therefore the similarity between two facial models f_1 and f_2 can be computed by the similarity of corresponding geodesics between the two models (corresponding geodesics on two facial models are shown in Fig.5). Angular index provides a correspondence between the geodesics on the face. The similarity of each pair of corresponding geodesics can be computed through the Fréchet distance between the two corresponding geodesics with the angle α incrementing on f_1 and f_2. The smaller the Fréchet distance of two curves is, the more similar the two curves are. The bigger the Fréchet distance is, the less similar the two curves are. Therefore, the similarity of two facial models can be defined by the average of Fréchet distances of all corresponding geodesics in the following equation.

$$d(f_1, f_2) = \frac{1}{m}\sum_{i=1}^{m} \delta_F(g^1_\alpha, g^2_\alpha).$$

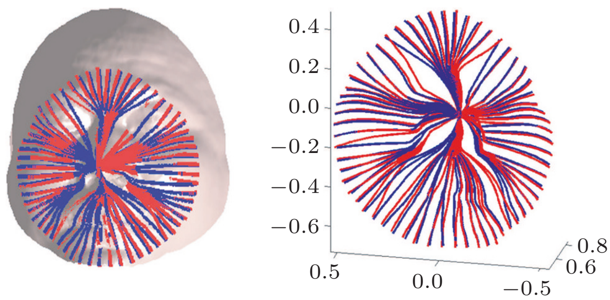

Fig.5. Corresponding geodesics on 3D facial models.

The average Fréchet distance can be computed approximately by the distance of coupling δ_{dF}, i.e.,

$$d(f_1, f_2) \approx \frac{1}{m}\sum_{i=1}^{m} \delta_{dF}(g^1_\alpha, g^2_\alpha).$$

The smaller the average Fréchet distance of two facial models $d(f_1, f_2)$ is, the more similar the two facial models are. On the contrary, the bigger the average Fréchet distance $d(f_1, f_2)$ is, the less similar they are. And we can prove $d(f_1, f_2)$ is a metric.

Theorem 1. *$d(f_1, f_2)$ is a metric.*

The proof is provided in Appendix.

In order to compare the similarity more intuitively, we define the similarity function $s : X \times X \to [0, 1]$ according to the average Fréchet distance by the following equation[2]:

$$s(f_1, f_2) = 1 - d(f_1, f_2)/d_{\max},$$

where $d_{\max}$ is the maximum average Fréchet distance. It is obvious that $s(f_1, f_2) \in [0, 1]$. 0 represents the two faces are completely different and 1 represents they are completely same. The bigger the value is, the more similar two faces are. And we also can prove that $s(f_1, f_2)$ satisfies three attributes: reflexivity, symmetry and triangle inequality.

Theorem 2. *The similarity s satisfies the following three attributes*:

1) *reflexivity*: $s(f_i, f_i) = 1$,

2) *symmetry*: $s(f_i, f_j) = s(f_j, f_i)$,

3) *triangle inequality properties*:

$s(f_i, f_j) \geqslant \max_k\{\max\{0, s(f_i, f_k) + s(f_j, f_k) - 1\}\}$.

We prove Theorem 2 in Appendix. The whole similarity measure algorithm of two facial models is shown in Algorithm 3.

5 Experimental Results

In order to validate our 3D facial similarity measure method based on the Fréchet distance of geodesics, we carry out the following experiments on open 3D face dataset GavaDB[30], Texas 3D Face Recognition database[31], and our face database① to verify whether our method effectively recognizes the facial models of the same person and reasonably measures the similarity of different persons' models.

5.1 Similarity Measure of Different Expressions or Poses Facial Models of the Same Person

First we select several models of the same person for similarity measure to verify whether the method can effectively distinguish different 3D face models of the same person with different people's 3D face models.

5.1.1 Experiments on GavaDB Database

GavaDB[30], a public database of 3D (three-dimensional) face database, provides 61 individual 3D face models (45 males and 16 females). Every person has nine different facial models in different expressions or poses, including six neutral expressions and three non-neutral expressions (smile, laugh and arbitrary expressions). Each of the 3D facial data is acquired by Minolta Vi-700 laser scanner and stored in a triangular mesh format. We select two models of each person. After facial models being preprocessed according to the method introduced in Section 2, the similarity of each two facial models can be computed by Algorithm 3 in Section 3.

Algorithm 3. 3D Facial Similarity Measure

Input: two 3D facial models f_1 and f_2

Output: the average of Fréchet distance $d(f_1, f_2)$ and similarity s

For $i = 1$ to 2 **do**

  Extract geodesic $G_i = \cup_\alpha g_\alpha^i (\alpha \in A)$

End

For $\alpha = 0$ to 2π **do**

  Compute $\delta_{dF}(g_\alpha^1, g_\alpha^2)$

End

Compute $d(f_1, f_2) \approx \frac{1}{m}\sum_{i=1}^{m} \delta_{dF}(g_\alpha^1, g_\alpha^2)$

Compute $s(f_1, f_2) = 1 - d(f_1, f_2)/d_{\max}$

The average Hausdorff distances and the average Fréchet distances of 3D facial models on GavaDB are listed in Table 1 and Table 2 respectively. All of the average distances computed by each two facial models shown in this paper are multiplied by 100. The values in bold represent the Fréchet distances and the Hausdorff distances of the same model are different. These values in Table 1 and Table 2 represent the similarity of different persons' facial models. We can see the average Fréchet distances are bigger than the average Hausdorff distances. It indicates the similarity values computed by the average Fréchet distances of different persons' faces are smaller than those computed by the average Hausdorff distances. Therefore, the average Fréchet distance can better reflect the face similarity.

As shown in Table 2, the diagonal average Fréchet distances between different facial models of the same person are far less than the values of the non-diagonal average Fréchet distances of different people's different facial models. This indicates that the similarity of two different 3D facial models of the same person is significantly higher than that of different people's different 3D facial models. Thus we compute the similarity values of 10 models of five persons in Fig.6 by the average Fréchet distances and the results are shown in Table 3. We can see that different facial models of the same person can be recognized correctly from Table 3.

Comparing our method with the iso-geodesics method proposed in [5] (the results are listed in Table 4), we can see that in our method the variation ranges of similarity values are bigger than those in the iso-geodesics method[5]. And our method has better discrimination ability than the iso-geodesics method[5].

①http://cist.bnu.edu.cn/yjycg/kytd/533.html, Sept. 2017.

Table 1. Average Hausdorff Distances of 3D Facial Models on GavaDB

	cara3_f1	cara4_f1	cara11_f1	cara14_f1	cara26_f1
cara3_f2	1.753 024 25	2.636 139 01	5.808 258 26	4.531 506 91	3.722 102 49
cara4_f2	2.652 112 83	1.385 016 90	3.925 646 63	**2.761 640 65**	2.166 300 04
cara11_f2	6.897 199 42	5.401 993 46	1.978 201 37	3.697 803 24	4.315 521 83
cara14_f2	**4.130 015 05**	2.813 992 07	**3.189 937 81**	2.031 402 06	**2.558 906 54**
cara26_f2	**3.398 707 65**	2.322 149 27	**3.090 112 72**	3.090 239 75	1.438 766 30

Note: All of the average distances computed by each two facial models shown in this paper are multiplied by 100. Diagonal data have been underlined where the distance between two faces is small and the similarity between them is high.

Table 2. Average Fréchet Distances of 3D Facial Models on GavaDB

	cara3_f1	cara4_f1	cara11_f1	cara14_f1	cara26_f1
cara3_f2	1.753 024 25	2.636 139 01	5.808 258 26	4.531 506 91	3.722 102 49
cara4_f2	2.652 112 83	1.385 016 90	3.925 646 63	**2.775 318 98**	2.166 300 04
cara11_f2	6.897 199 42	5.401 993 46	1.978 201 37	3.697 803 24	4.315 521 83
cara14_f2	**4.130 250 74**	2.813 992 07	**3.190 560 89**	2.031 402 06	**2.559 220 51**
cara26_f2	**3.399 717 47**	2.322 149 27	**3.090 189 06**	3.099 614 45	1.438 766 30

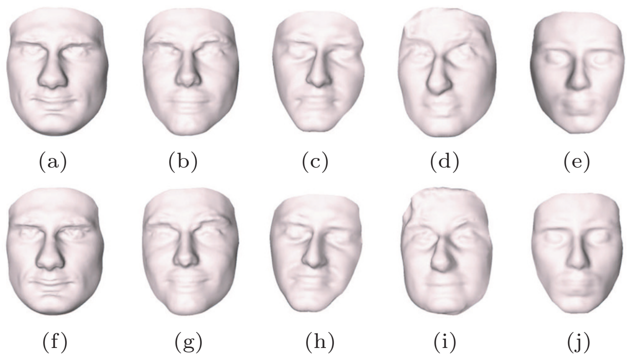

Fig.6. 3D models in GavaDB dataset. (a) cara3_f1. (b) cara4_f1. (c) cara11_f1. (d) cara14_f1. (e) cara26_f1. (f) cara3_f2. (g) cara4_f2. (h) cara11_f2. (i) cara14_f2. (j) cara26_f2.

Table 3. Similarity of 3D Facial Models on GavaDB Using the Average Fréchet Distances of Geodesics

	cara3_f1	cara4_f1	cara11_f1	cara14_f1	cara26_f1
cara3_f2	0.745 8	0.617 8	0.157 9	0.343 0	0.460 3
cara4_f2	0.615 5	0.799 2	0.430 8	0.597 6	0.685 9
cara11_f2	0.000 0	0.216 8	0.713 2	0.463 9	0.374 3
cara14_f2	0.401 2	0.592 0	0.537 4	0.705 5	0.628 9
cara26_f2	0.507 1	0.663 3	0.552 0	0.550 6	0.791 4

Table 4. Similarity of 3D Facial Models on GavaDB Using iso-Geodesics[5]

	cara3_f1	cara4_f1	cara11_f1	cara14_f1	cara26_f1
cara3_f2	0.916 2	0.901 4	0.867 8	0.881 5	0.882 9
cara4_f2	0.874 0	0.957 1	0.817 6	0.871 2	0.914 0
cara11_f2	0.834 2	0.874 7	0.874 5	0.851 7	0.838 3
cara14_f2	0.891 3	0.857 7	0.829 7	0.896 9	0.815 0
cara26_f2	0.805 9	0.883 8	0.798 5	0.814 7	0.953 0

5.1.2 Experiments on Texas 3D Face Recognition Database

The Texas 3D Face Recognition database contains 1 149 pairs of high resolution, pose normalized, preprocessed, and perfectly aligned color and range images of 118 adults[31]. The data are acquired by an MU-2 stereo imaging system and include the range images of one person in different poses, expressions or illuminations. In order to do experiments on them using our method, the 3D point cloud data are generated from the range images by making the gray value as the third dimension coordinate value. Then the point cloud data are triangulated into mesh models. Lastly, the face mesh models are pretreated, including de-noising, filling-up holes, and so on. Thus geodesics can be extracted from them and the similarity can be computed by our 3D face similarity measure method based on Fréchet distances of geodesics. Twelve facial models of six persons in different expressions or poses are shown in Fig.7.

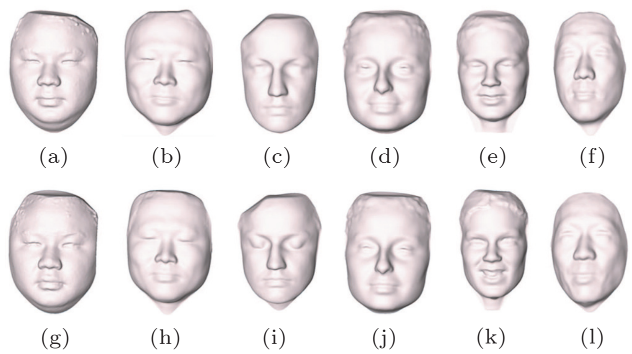

Fig.7. 3D models for comparison in Texas 3D face recogniton database. (a) 0003_003. (b) 0120_063. (c) 0290_096. (d) 0043_025. (e) 0385_100. (f) 0716_109. (g) 0004_003. (h) 0121_063. (i) 0291_096. (j) 0045_025. (k) 0389_100. (l) 0698_109.

The average Hausdorff distances and the average Fréchet distances of 3D facial models on the Texas 3D Face Recognition database are listed in Table 5 and Table 6 respectively. The values in bold represent the average Fréchet distances and the average Hausdorff distances are different. These values in Table 5 and Table 6 represent the similarity of different persons' facial models. We can see the average Fréchet distance is bigger than the average Hausdorff distance especially of the faces 0043_025 and 0385_100 which have expression variations. It indicates the similarity values computed by the average Fréchet distances of different persons' facial models are smaller than those computed by the average Hausdorff distances. Therefore the average Fréchet distance can better reflect the face similarity especially in the situation of expression variations.

From Table 6, we can see that the average Fréchet distances on the diagonal between different facial models of the same person are far less than the average Fréchet distances on the non-diagonal of different peoples' facial models. This indicates that the similarity of two different 3D facial models of the same person is significantly higher than the similarity of different people's 3D facial models. Therefore we compute the similarity values of 12 models of six persons in Fig.7 by the average Fréchet distances and results are shown in Table 7. From Table 7 we can see that the same person, when his(her) facial models with different poses or facial expressions are given, can be recognized correctly.

Comparing our method with the iso-geodesics method[5] on the Texas 3D Face Recognition database (the results are listed in Table 8), we can see that the similarity values computed by the iso-geodesics method are entirely high and the similarity values computed by our method are more reasonable than those by the iso-geodesics method[5]. And our method has better discrimination ability than the iso-geodesics method[5].

5.2 Similarity Measure of Different Persons' 3D Facial Models

3D facial similarity measure should not only distinguish the models of the same person from different person's models, but also give the correct similarity value of 3D facial models of different persons. Since face similarity is an ambiguous and relative concept, we verify our method through two experiments on two kinds of data: one is on morph data and the other is on real face models of different persons.

Table 5. Average Hausdorff Distances of 3D Facial Models on Texas 3D Face Data

	0003_003	0120_063	0290_096	0043_025	0385_100	0716_109
0004_003	2.346 831 13	3.769 986 68	**10.722 253 60**	**4.960 814 01**	**5.068 503 85**	**4.165 097 97**
0121_063	**2.995 388 68**	1.036 200 83	**12.234 402 49**	**4.361 143 59**	**6.199 648 31**	3.954 155 17
0291_096	**11.461 627 87**	**11.754 399 33**	2.100 707 27	**10.365 793 66**	**8.647 882 04**	**10.471 248 02**
0045_025	4.651 543 30	**4.713 032 21**	**10.301 875 08**	1.589 583 39	**4.104 259 58**	**4.312 004 96**
0389_100	**5.755 329 00**	6.159 988 67	**9.701 574 72**	4.331 059 88	1.643 818 74	**4.287 058 55**
0698_109	**4.075 903 48**	3.843 766 04	**10.680 362 85**	**4.103 569 67**	**4.334 569 51**	1.234 500 03

Table 6. Average Fréchet Distances of 3D Facial Models on Texas 3D Face Data

	0003_003	0120_063	0290_096	0043_025	0385_100	0716_109
0004_003	2.346 843 10	3.769 986 68	**12.794 008 83**	**4.960 927 29**	**5.068 514 90**	**4.165 147 87**
0121_063	**2.995 995 28**	1.036 200 83	**14.227 383 95**	**4.361 261 61**	**6.199 653 59**	3.954 155 17
0291_096	**13.554 232 66**	**13.796 232 12**	2.100 707 27	**12.289 481 11**	**10.698 115 67**	**12.596 277 43**
0045_025	4.651 543 30	**4.713 085 49**	**12.241 238 35**	1.589 583 39	**4.104 307 96**	**4.312 184 93**
0389_100	**5.755 380 38**	6.159 988 67	**11.763 719 90**	4.331 059 88	1.643 818 74	**4.288 129 57**
0698_109	**4.075 960 59**	3.843 766 04	**12.766 941 15**	**4.103 582 06**	**4.334 574 27**	1.234 502 43

Table 7. Similarity of 3D Facial Models on Texas 3D Face Data Using Average Fréchet Distances of Geodesics

	0003_003	0120_063	0290_096	0043_025	0385_100	0716_109
0004_003	0.835 047	0.735 019	0.100 748	0.651 311	0.643 749	0.707 244
0121_063	0.789 421	0.927 169	0.000 000	0.693 460	0.564 245	0.722 074
0291_096	0.047 314	0.030 304	0.852 348	0.136 209	0.248 062	0.114 646
0045_025	0.673 057	0.668 731	0.139 600	0.888 273	0.711 521	0.696 909
0389_100	0.595 472	0.567 033	0.173 164	0.695 583	0.884 461	0.698 600
0.698_109	0.713 513	0.729 833	0.102 650	0.711 572	0.695 336	0.913 231

Note: Two facial models of the same person have the same last three numbers, for example, 0003_003 and 0004_003 are the facial models of the same person.

Table 8. Similarity of 3D Facial Models on Texas 3D Face Data Using iso-Geodesics[5]

	0003_003	0120_063	0290_096	0043_025	0385_100	0716_109
0004_003	0.973 5	0.931 8	0.894 9	0.902 2	0.947 7	0.852 6
0121_063	0.899 7	0.996 1	0.871 0	0.872 2	0.927 3	0.854 5
0291_096	0.902 0	0.875 8	0.990 4	0.959 9	0.921 0	0.910 0
0045_025	0.903 8	0.873 3	0.963 8	0.985 7	0.912 0	0.931 6
0389_100	0.952 7	0.900 7	0.905 1	0.909 7	0.975 7	0.845 4
0698_109	0.864 5	0.872 5	0.929 4	0.924 5	0.888 9	0.980 7

5.2.1 *Experiments on Morph Data*

The basic idea of this experiment is to generate several morph deformed facial models from two real facial models which can be known the similarity between each two faces in advance. Therefore we can verify whether the similarity calculated by our method is correct or not. We randomly select two 3D facial models f_1 and f_2, and then generate morph deformed facial models by the following equation reference[6].

$$f_i = (1-\lambda)f_1 + \lambda f_2.$$

The degree of two faces mixed is controlled by parameter λ. If $\lambda = 0$, the generated facial model is the same with f_1. And if $\lambda = 1$, the generated facial model is the same with f_2. The face generated by $\lambda = 0.25$ should be closer to f_1 than the face generated by $\lambda = 0.75$. The facial models in the first row and column in Fig.8 show the three new generated facial models "new_1", "new_2" and "new_3" by f_1 and f_2 according to the above morph deformation method, corresponding to $\lambda = \{0.25, 0.50, 0.75\}$ respectively.

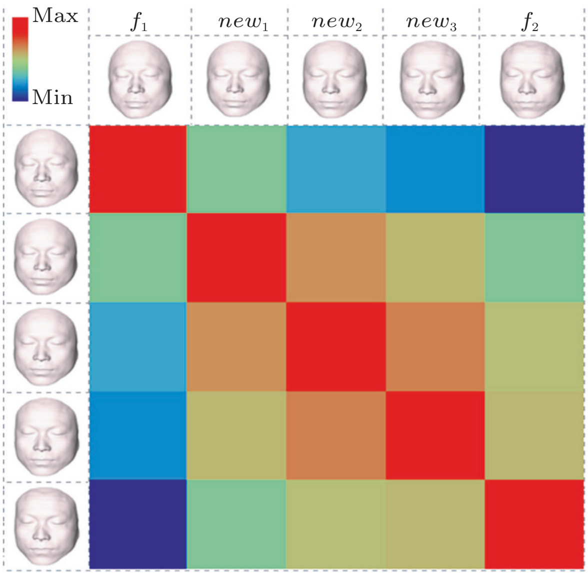

Fig.8. Similarity diagram of deformed facial models by f_1 and f_2.

The average Hausdorff distances and the average Fréchet distances of different persons' 3D facial models on the above Morph data are listed in Table 9 and Table 10 respectively. The values in bold represent the average Fréchet distances and the average Hausdorff distances are different. These values in Table 9 and Table 10 represent the similarity of different persons' facial models. We can see the average Fréchet distances are bigger than the average Hausdorff distances. It indicates the similarity values computed by the average Fréchet distances of different persons' 3D facial models are smaller than those computed by the average Hausdorff distances. Therefore the average Fréchet distance can better reflect the face similarity.

The similarity between each two facial models can be computed by our method based on the average Fréchet distances of geodesics which are listed in Table 10 and similarity values are listed in Table 11. The color diagram is drawn in Fig.8, where the red color represents the maximum (max) similarity value and the blue color indicates the minimum (min) similarity value in order to show the laws of the similarity intuitively.

Table 9. Average Hausdorff Distances of Morph Data

	f_1	new_1	new_2	new_3	f_2
f_1	0.000 0	**3.404 0**	**4.732 1**	**5.224 3**	**7.169 3**
new_1	**3.404 0**	0.000 0	1.940 4	**2.735 0**	4.391 5
new_2	**4.732 1**	1.940 4	0.000 0	1.638 2	2.916 2
new_3	**5.224 3**	**2.735 0**	1.638 2	0.000 0	**2.730 5**
f_2	**7.169 3**	4.391 5	2.916 2	**2.730 5**	0.000 0

Table 10. Average Fréchet Distances of Morph Data

	f_1	new_1	new_2	new_3	f_2
f_1	0.000 0	**4.385 8**	**5.715 2**	**6.207 4**	**8.154 3**
new_1	**4.385 8**	0.000 0	1.940 4	**2.735 4**	4.391 5
new_2	**5.715 2**	1.940 4	0.000 0	1.638 2	2.916 2
new_3	**6.207 4**	**2.735 4**	1.638 2	0.000 0	**2.730 6**
f_2	**8.154 3**	4.391 5	2.916 2	**2.730 6**	0.000 0

Table 11. Similarity of Morph Data Using Average Fréchet Distances of Geodesics

	f_1	new_1	new_2	new_3	f_2
f_1	1.000 0	0.462 1	0.299 1	0.238 8	0.000 0
new_1	0.462 1	1.000 0	0.762 0	0.664 5	0.461 4
new_2	0.299 1	0.762 0	1.000 0	0.799 1	0.642 4
new_3	0.238 8	0.664 5	0.799 1	1.000 0	0.665 1
f_2	0.000 0	0.461 4	0.642 4	0.665 1	1.000 0

From Table 10, Table 11 and Fig.8, we can see that the average Fréchet distances in the diagonal are the minimum value 0 which reflects they have the maximum similarity 1 because they are the same models. At the same time, the average Fréchet distance and similarity value between "f_1" and "f_2" is the same with "f_2" and "f_1", and it reflects the similarity matrix is symmetric. In addition, the trend of the average Fréchet distance value between the faces "new_1", "new$_2$", "new$_3$", "f_2" and the face "f_1" is sequentially increasing, and it indicates that the similarity values of them are sequentially decreasing. Therefore the color gradually changes from the red to the blue. And the variation trend of similarity value is consistent with the parameter values used by morph deformation face, and also consistent with a person's subjective judgment. The similarities of other faces have the same laws. This illustrates that the similarity computed by our method based on the average Fréchet distances is reasonable. And it can correctly give the quantitative similarity values of different persons' face models.

Comparing our method with the iso-geodesics method[5] (the results are listed in Table 12), we can see that the similarity values computed by the iso-geodesics method are entirely high and have poor discrimination. In our method the variation ranges of similarity values are bigger than those in the iso-geodesics method[5]. And our method has better discrimination ability than the iso-geodesics method[5].

Table 12. Similarity of Morph Data Using iso-Geodesics[5]

	f_1	new_1	new_2	new_3	f_2
f_1	1.000 0	0.989 6	0.972 6	0.958 2	0.941 0
new_1	0.989 6	1.000 0	0.994 9	0.986 1	0.968 5
new_2	0.972 6	0.994 9	1.000 0	0.996 9	0.983 0
new_3	0.958 2	0.986 1	0.996 9	1.000 0	0.989 2
f_2	0.941 0	0.968 5	0.983 0	0.989 2	1.000 0

5.2.2 *Experiments on Real 3D Face Data*

The real 3D face dataset is from VRVT (virtual reality and visualization technology) Lab of Beijing Normal University②. There are pairs of craniofacial skull and skin data scanned by CT (computed tomography). The data come from 208 adult live persons, aged from 19 to 75 years old. The 3D facial models have been reconstructed by original CT images. After preprocessing the 3D facial models by the method presented in Section 2, the average Hausdorff distance and the average Fréchet distance are calculated for the extracted geodesics on each pair of 3D facial models. Take the model number 008-1829 for example, the comparison results between it and other models are shown in Table 13.

In Table 13, all the values of different persons' 3D facial models in bold represent the average Fréchet distances and the average Hausdorff distances are different. We can see the average Fréchet distances are all bigger than the average Hausdorff distances. It indicates the similarity values computed by the average Fréchet distances are smaller than those computed by the average Hausdorff distances. Therefore the average Fréchet distances can better reflect the face similarity and have a better distinction ability. Thus we compute the similarity by the average Fréchet distances which are listed in the bottom line of Table 13.

In the models shown in Table 13, the average Fréchet distance between the model with number 008-1829 and the model with number 008-2604 is the smallest. This indicates that these two 3D models have the highest similarity and it is in accordance with people's subjective observation.

Table 13. Comparison of 3D Facial Models of Different Persons Using the Average Fréchet Distances of Geodesics

	008-1829	008-2604	024-10	007-5019	010-5904	003-4344	23892
							
Average Hausdorff distance ($d \times 10^2$)	**0**	**2.895 5**	**7.333 6**	**6.982 0**	**10.324 0**	**10.920 3**	**11.640 2**
Average Fréchet distance ($d \times 10^2$)	**0**	**2.895 8**	**7.334 0**	**6.985 9**	**12.172 3**	**12.793 2**	**13.543 7**
Similarity	1	0.806 5	0.509 9	0.533 2	0.186 6	0.145 1	0.095 0

②http://cist.bnu.edu.cn/yjycg/kytd/533.html, Sept. 2017.

And the average Fréchet distances between the 3D facial models 008-1829 and 024-10, 008-1829 and 007-5019, 008-1829 and 010-5904 are smaller than the average Fréchet distances between the 3D facial models 008-1829 and 003-4344, 008-1829 and 23892. It indicates that the first three facial models are more similar to the facial model 008-1829 than the latter two facial models (003-4344, 23892). This is also consistent with people's subjective evaluation. Therefore the method based on the Fréchet distances of geodesics can reasonably measure the similarity of different persons' face models.

6 Conclusions

In this paper, we proposed a novel 3D human face similarity measure method by Fréchet distances of geodesics extracted from 3D facial models. In our method, the surface comparison of 3D faces is converted into a set of 3D curves comparison on face surface. Considering the Fréchet distance is an effective metric for measuring curve similarity, we firstly introduced it to measure face similarity. Due to the intrinsic property of geodesic, we selected geodesics as the comparison curves. Firstly, the geodesics on each 3D facial model emanated from the nose tip point are extracted in equal angular increment. Secondly, the Fréchet distances of the corresponding geodesics on two compared facial models are computed. At last, the similarity of two facial models is computed based on the average Fréchet distances of the geodesics extracted from them.

Experiments were performed on the open 3D face database GavaDB, the Texas 3D Face Recognition database, and our 3D face database, including morph data and real 3D face data. The results illustrated that by our method based on Fréchet distances of the geodesics, the similarity of different 3D facial models of the same person is higher than the similarity of different persons' 3D facial models. And the similarity values of different persons' 3D facial models are consistent with people's subjective evaluation. These indicated that our method can not only identify the same person when his(her) facial models with different poses or facial expressions are given, but also reflect the quantitative similarity values of different persons' face models.

In the future, on one hand, we will compute the geodesic distance by more robust and faster algorithms[32-33] to improve our geodesic algorithm's efficiency and robustness. On the other hand, we will do more experiments on more 3D face models in the public datasets and apply our method to 3D face recognition.

Acknowledgement(s) The authors gratefully appreciate the anonymous reviewers for all of their helpful comments, professors Alan C. Bovik and Shalini Gupta for providing the data of Texas 3D Face Recognition database, and the providers of GavaDB dataset. They also thank Surazhsky *et al.* and Eiter *et al.* for their public codes of geodesic distance and Fréchet distance respectively, which are used in our method.

References

[1] Daoudi M, Srivastava A, Veltkamp R. 3D Face Modeling, Analysis and Recognition. John Wiley & Sons, 2013.

[2] Adan A, Adan M. A flexible similarity measure for 3D shapes recognition. *IEEE Trans. Pattern Analysis and Machine Intelligence*, 2004, 26(11): 1507-1520.

[3] Stephan C N, Arthur R S. Assessing facial approximation accuracy: How do resemblance ratings of disparate faces compare to recognition tests? *Forensic Science International*, 2006, 159(Suppl 1): S159-S163.

[4] Quatrehomme G, Balaguer T, Staccini P, Alunni-Perret V. Assessment of the accuracy of three-dimensional manual craniofacial reconstruction: A series of 25 controlled cases. *International Journal of Legal Medicine*, 2007, 121(6): 469-475.

[5] Li H Y, Wu Z K, Zhou M Q. A iso-geodesic stripes based similarity measure method for 3D face. In *Proc. the 4th Int. Conf. Biomedical Engineering and Informatics* (*BMEI*), October 2011, pp.2114-2118.

[6] Moorthy A K, Mittal A, Jahanbin S, Grauman K, Bovik A C. 3D facial similarity: Automatic assessment versus perceptual judgments. In *Proc. the 4th IEEE Int. Conf. Biometrics: Theory Applications and Systems* (*BTAS*), September 2010.

[7] Bowyer K W, Chang K, Flynn P. A survey of approaches and challenges in 3D and multi-modal 3D + 2D face recognition. *Computer Vision and Image Understanding*, 2006, 101(1): 1-15.

[8] Scheenstra A, Ruifrok A, Veltkamp R C. A survey of 3D face recognition methods. In *Proc. the 5th Int. Conf. Audio-and Video-Based Biometric Person Authentication*, July 2005, pp.891-899.

[9] Nagamine T, Uemura T, Masuda I. 3D facial image analysis for human identification. In *Proc. the 11th IAPR Int. Conf. Pattern Recognition, Computer Vision and Applications*, September 1992, pp.324-327.

[10] Wu Y J, Pan G, Wu Z H. Face authentication based on multiple profiles extracted from range data. In *Proc. the 4th Int. Conf. Audio- and Video-Based Biometric Person Authentication*, Jun. 2003, pp.515-522.

[11] ter Haar F B, Veltkampy R C. SHREC' 08 entry: 3D face recognition using facial contour curves. In *Proc. IEEE Int. Conf. Shape Modeling and Applications*, June 2008, pp.259-260.

[12] Jahanbin S, Choi H, Liu Y, Bovik A C. Three dimensional face recognition using iso-geodesic and iso-depth curves. In *Proc. the 2nd IEEE Int. Conf. Biometrics: Theory, Applications and Systems*, October 2008.

[13] Bronstein A M, Bronstein M M, Kimmel R. Three-dimensional face recognition. *International Journal of Computer Vision*, 2005, 64(1): 5-30.

[14] Berretti S, Del Bimbo A, Pala P. Description and retrieval of 3D face models using iso-geodesic stripes. In *Proc. the 8th ACM Int. Workshop on Multimedia Information Retrieval*, October 2006, pp.13-22.

[15] Berretti S, Del Bimbo A, Pala P. 3D face recognition using iso-geodesic stripes. *IEEE Trans. Pattern Analysis and Machine Intelligence*, 2010, 32(12): 2162-2177.

[16] Mpiperis I, Malassiotis S, Strintzis M G. 3-D face recognition with the geodesic polar representation. *IEEE Trans. Information Forensics and Security*, 2007, 2(3): 537-547.

[17] Achermann B, Bunke H. Classifying range images of human faces with hausdorff distance. In *Proc. the 15th Int. Conf. Pattern Recognition*, September 2000, pp.809-813.

[18] Lee Y H, Shim J C. Curvature based human face recognition using depth weighted hausdorff distance. In *Proc. Int. Conf. Image Processing*, October 2004, pp.1429-1432.

[19] Shahbaz K. Applied similarity problems using Fréchet distance [Ph.D. Thesis]. Carleton University, Ottawa, 2013.

[20] Hu Y L, Duan F Q, Yin B C, Zhou M Q, Sun Y F, Wu Z K, Geng G H. A hierarchical dense deformable model for 3D face reconstruction from skull. *Multimedia Tools and Applications*, 2013, 64(2): 345-364.

[21] Mitchell J S B, Mount D M, Papadimitriou C H. The discrete geodesic problem. *SIAM Journal on Computing*, 1987, 16(4): 647-668.

[22] Xin S Q, Wang G J. Improving Chen and Han's algorithm on the discrete geodesic problem. *ACM Trans. Graphics (TOG)*, 2009, 28(4): Article No. 104.

[23] Ying X, Xin S Q, He Y. Parallel Chen-Han (PCH) algorithm for discrete geodesics. *ACM Trans. Graphics (TOG)*, 2014, 33(1): Article No. 9.

[24] Ying X, Wang X N, He Y. Saddle vertex graph (SVG): A novel solution to the discrete geodesic problem. *ACM Trans. Graphics (TOG)*, 2013, 32(6): Article No. 170.

[25] Surazhsky V, Surazhsky T, Kirsanov D, Gortler S J, Hoppe H. Fast exact and approximate geodesics on meshes. *ACM Trans. Graphics (TOG)*, 2005, 24(3): 553-560.

[26] Fréchet M M. Sur quelques points du calcul fonctionnel. *Rendiconti del Circolo Matematico di Palermo (1884-1940)*, 1906, 22(1): 1-72. (in German)

[27] Alt H, Godau M. Computing the Fréchet distance between two polygonal curves. *International Journal of Computational Geometry & Applications*, 1995, 5(01n02): 75-91.

[28] Rote G. Computing the Fréchet distance between piecewise smooth curves. *Computational Geometry: Theory and Applications*, 2007, 37(3): 162-174.

[29] Eiter T, Mannila H. Computing discrete Fréchet distance. Technical Report CD-TR 94/64. http://citeseerx.ist.psu.edu/viewdoc/download?doi = 10.1.1.4.5330&rep=rep1&type=pdf, April 1994.

[30] Moreno A, Sánchez A. GavabDB: A 3D face database. In *Proc. the 2nd COST Workshop on Biometrics on the Internet*, March 2004, pp.75-80.

[31] Gupta S, Castleman K R, Markey M K, Bovik A C. Texas 3D face recognition database. In *Proc. IEEE Southwest Symp. Image Analysis & Interpretation (SSIAI)*, May 2010, pp.97-100.

[32] Liu Y J. Exact geodesic metric in 2-manifold triangle meshes using edge-based data structures. *Computer-Aided Design*, 2013, 45(3): 695-704.

[33] Xu C X, Wang T Y, Liu Y J, Liu L G, He Y. Fast Wavefront Propagation (FWP) for computing exact geodesic distances on meshes. *IEEE Trans. Visualization and Computer Graphics*, 2015, 21(7): 822-834.

Jun-Li Zhao is an associate professor and master supervisor in School of Data Science and Software Engineering, Qingdao University, Qingdao. She received her Ph.D. degree in computer applied technology in 2015 from Beijing Normal University, Beijing. She is a member of CCF. She is currently engaged in postdoctoral research on computer graphics, computer vision, and virtual reality research.

Zhong-Ke Wu is a full professor in College of Information Science and Technology, Beijing Normal University (BNU), Beijing. Prior to joining in BNU, he worked in Nanyang Technological University (NTU), Singapore, Institute National de Recherche en Informatique et en Automatique (INRIA) in France, Institute of High Performance Computing (IHPC), Singapore, and Institute of Software, Chinese Academy of Sciences, Beijing, from 1995 to 2006. Prof. Wu has been working in the field of computer graphics since 1988. His current research interests include computer graphics, animation virtual reality, geometric modeling, volume graphics, and medical imaging.

Zhen-Kuan Pan is a professor in College of Computer Science and Technology, Qingdao University, Qingdao. He received his Ph.D. degree in mechanics from Shanghai Jiao Tong University, Shanghai, in 1992. He was a visiting scholar of University of California, Los Angeles. His main research interests focus on computer vision, image processing, multi-body system dynamics and control.

Fu-Qing Duan received his Ph.D. degree in 2006 from the National Laboratory of Pattern Recognition (NLPR) at the Institute of Automation of the Chinese Academy of Sciences (CAS), Beijing. Currently, he is a professor at the College of Information Science and Technology, Beijing Normal University, Beijing. His research interests are computer vision and computer graphics.

Jin-Hua Li received his Ph.D. degree in computer science (Dr. rer. nat.) from Stuttgart University, Germany, in 1998. He is currently a professor of Qingdao University, Qingdao. He received a scholarship from DAAD (German Academic Exchange Service) and worked as Ph.D. candidate in the Institute of Computer Science, Stuttgart University, in 1993~1999. His research interests include software development methodology, computer languages, empirical software engineering, formal methods, science and techniques of big data. He has published over 50 science papers and six textbooks in Chinese. Dr. Li is a member of CCF. He has been a PC member of QuASoQ since 2014.

Zhi-Han Lv is an engineer and researcher in virtual/augmented reality and multimedia, with a major in mathematics and computer science, having plenty of work experience in virtual reality and augmented reality projects, and is engaged in the application of computer visualization and computer vision. Zhi-Han Lv received his Ph.D. degree in computer applied technology from Ocean University of China, Qingdao, in 2012. His research application fields range widely, from everyday life to traditional research fields (geography, biology, medicine).

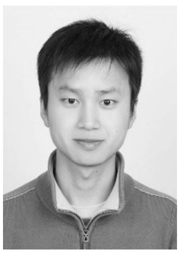

Kang Wang received his Ph.D. degree in systems analysis and integration from the Institute of Virtual Reality and Visualization in 2015 from Beijing Normal University, Beijing. His research interests include computer graphics, geometric modeling and differential geometry. He is a lecturer of Capital Normal University, Beijing.

Yu-Cong Chen is a Ph.D. student in College of Information Science and Technology in Beijing Normal University, Beijing. His research interests include computer vision and computer graphics.

Appendix

Proof of Theorem 1. Eiter and Mannila[29] proofed that δ_{dF} is a metric, and it satisfies the following three attributes:

1) nonnegativity: $\delta_{dF}(g^1, g^2) \geqslant 0$,

$$\delta_{dF}(g^1, g^2) = 0 \text{ only if } g^1 = g^2;$$

2) symmetry:

$$\delta_{dF}(g^1, g^2) = \delta_{dF}(g^2, g^1);$$

3) triangle inequality property:

$$\delta_{dF}(g^1, g^3) \leqslant \delta_{dF}(g^1, g^2) + \delta_{dF}(g^2, g^3).$$

Next, we will prove $d(f_1, f_2)$ also satisfies the properties of nonnegativity, symmetry, and triangle inequality. Nonnegativity and symmetry can be proved easily. Thus we prove triangle inequality only.

Because δ_{dF} is a metric, we can deduce the following equation:

$$\begin{aligned} & \frac{1}{m}\sum_{i=1}^{m} \delta_{dF}(g_i^1, g_i^2) + \frac{1}{m}\sum_{i=1}^{m} \delta_{dF}(g_i^2, g_i^3) \\ = & \frac{1}{m}\sum_{i=1}^{m} (\delta_{dF}(g_i^1, g_i^2) + \delta_{dF}(g_i^2, g_i^3)) \\ \geqslant & \frac{1}{m}\sum_{i=1}^{m} \delta_{dF}(g_i^1, g_i^3). \end{aligned}$$

According to the definition of $d(f_1, f_2)$, we can deduce that

$$d(f_1, f_2) + d(f_2, f_3) \geqslant d(f_1, f_3). \qquad \square$$

Proof of Theorem 2.

1) Reflexivity:

$\because d(f_1, f_2) = 0$ only if $f_1 = f_2$,
$\therefore d(f_i, f_i) = 0$,
$\therefore s(f_i, f_i) = 1 - d(f_i, f_i)/d_{\max} = 1 - 0/d_{\max} = 1$.

2) Symmetry:

$$\begin{aligned} s(f_i, f_j) &= 1 - d(f_i, f_j)/d_{\max} \\ &= 1 - d(f_j, f_i)/d_{\max} \\ &= s(f_j, f_i), \end{aligned}$$

3) Triangle inequality properties:

$$\begin{aligned} &\max_k\{\max\{0, s(f_i, f_k) + s(f_j, f_k) - 1\}\} \\ &= \max_k\{\max\{0, 1 - \frac{d(f_i, f_k)}{d_{\max}} + 1 - \frac{d(f_j, f_k)}{d_{\max}} - 1\}\} \\ &= \max_k\{\max\{0, 1 - \frac{d(f_i, f_k)}{d_{\max}} - \frac{d(f_j, f_k)}{d_{\max}}\}\} \\ &= \max_k\{\max\{0, 1 - \frac{(d(f_i, f_k) + d(f_j, f_k))}{d_{\max}}\}\} \\ &\leqslant \max\{0, 1 - \frac{d(f_i, f_j)}{d_{\max}}\} \\ &= \max\{0, s(f_i, f_j)\} \\ &= s(f_i, f_j). \end{aligned}$$

□